USING BENDER ELEMENTS TO DETERMINE ELASTIC SOIL PARAMETERS

Meyer, V. M. and Pender, M. J.

Department of Civil and Resource Engineering
The University of Auckland, New Zealand

SUMMARY

This paper presents results from several bender element tests performed on undisturbed samples of differing soil type. The bender elements enabled both P- and S-wave velocities to be measured. Using the theory of elastic wave propagation, the dynamic elastic parameters G_{max}, E, and ν for the soil samples were evaluated. These parameters showed general agreement with soil type.

INTRODUCTION

The three basic constants of the theory of elasticity are E, G and ν, where E is the modulus of elasticity (Young's modulus), G is the shear modulus of elasticity and ν is Poisson's ratio. These constants are essential parameters in the design and low strain analysis of many geotechnical applications. However, the non-linear inelastic behaviour of soil does not readily lend itself toward experimental determination of these elastic properties.

The small strain shear modulus (G_{max} or G_o) of a soil is associated with shear strains (typically < 10^{-3}%) at which the soil can be considered to behave in an elastic manner. This condition is represented by the maximum shear modulus being invariant with shear strain, as shown by the *strain plateau* in Figure 1.

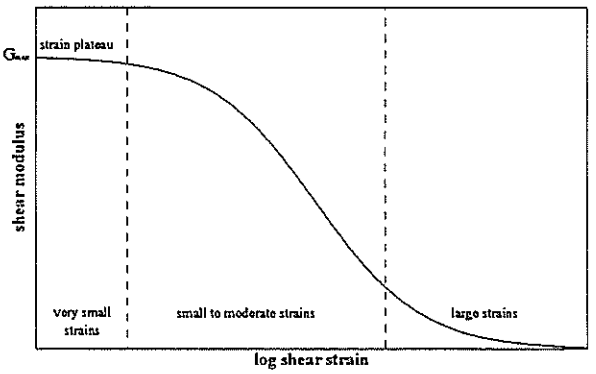

Figure 1 - Shear modulus variation with shear strain

G_{max} is commonly evaluated through dynamic in situ or laboratory testing. In situ tests commonly include down-hole (or up-hole) and cross-hole seismic tests. Laboratory tests include dynamic strain or stress controlled triaxial tests, resonant column tests, free vibration torsion tests and bender element tests.

This paper deals with the bender element method of determining G_{max}, though the following theory is equally applicable to in situ seismic methods.

THEORY OF ELASTIC WAVE PROPAGATION

Seismic methods of determining G_{max} are based on the fact that the velocity at which seismic waves travel through a medium is dependent upon the elastic properties of the material. From the theory of plane wave propagation in a homogeneous isotropic elastic material, it can be shown that two types of body waves propagate. The first type is a compressional wave (P-wave), which propagates with a velocity v_p, given by:

$$v_p^2 = \frac{E(1-\nu)}{\rho(1+\nu)(1-2\nu)} \tag{1}$$

where ρ is mass density, E is the modulus of elasticity, G is the shear modulus of elasticity and ν is Poisson's ratio.

The second type of body wave is a shear wave (S-wave), which propagates with a velocity, v_s, given by:

$$v_s^2 = G/\rho \tag{2}$$

Comparison of equations (1) and (2) reveal that, for the same material parameters, P-waves propagate at a much faster velocity than S-waves, with the difference between the velocities dependent upon the value of Poisson's ratio.

Measurements of v_p and v_s can be made by generating a seismic disturbance at a specific point and recording the time required for the disturbance to reach one or more receivers positioned in the medium. If the distance travelled by the body waves is known, it is possible to calculate v_p and v_s respectively. It is common practice to reverse the polarity of the seismic disturbance, which correspondingly reverses the polarity of the received signal. This enables the first arrival of the shear wave to be more clearly defined (Abbiss [1]).

The dynamic elastic parameters G_{max}, E and ν can be evaluated if the mass density, ρ, v_p and v_s of the medium are known, since:

$$G = \frac{E}{2(1+\nu)} \tag{3}$$

Using equations (3), (2) and (1) it can be shown that:

$$\nu = \frac{\frac{1}{2}\left(v_p/v_s\right)^2 - 1}{\left(v_p/v_s\right)^2 - 1} \tag{4}$$

A ν value approaching 0.5, corresponds to a very large bulk modulus, or a condition of zero volume change (ie an undrained test). This criteria may well be satisfied for bender element tests on a saturated clay with a low value of G_{max} and a high P-wave velocity.

PIEZOCERAMIC BENDER ELEMENTS

A bender element is a small transducer comprised of two thin piezoceramic plates rigidly bound together in a sandwich type arrangement. The configuration of the ceramic material is such that it enables the bender element to convert electrical energy in to mechanical energy and vice-versa. Hence, an applied voltage causes the bender element to bend or deflect a small amount, and conversely, the bender element generates a small voltage as it bends. Figure 2 shows a bender element before and after an excitation voltage is applied.

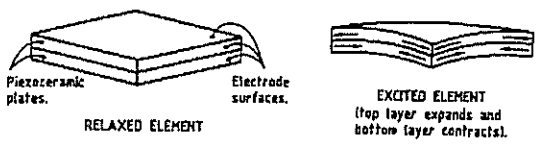

Figure 2 - Shape of piezoceramic bender element before and after application of excitation voltage (after Dyvik and Madshus [2])

The use of bender elements to measure the shear wave velocity of soil in laboratory specimens has been described in detail by Dyvik and Madshus [2]. Test results presented in this paper were obtained by mounting bender elements in a triaxial cell using the techniques developed by Dyvik and Madshus. A brief summary of the techniques employed is given below.

The bender element must be protected from moisture to prevent electrical shorting of the transducer. This was achieved by encasing the bender elements in an epoxy resin. The encased bender elements were then mounted in both the top and bottom end platens, as shown in Figure 3.

A porous disc with a corresponding slot could be mounted over the bender element if required. The slot in the porous disc was large enough to ensure that it did not interfere with the operation of the bender element. The resultant length of bender element protruding in to the soil specimen was of the order 9.5mm with the porous disc and 11mm without.

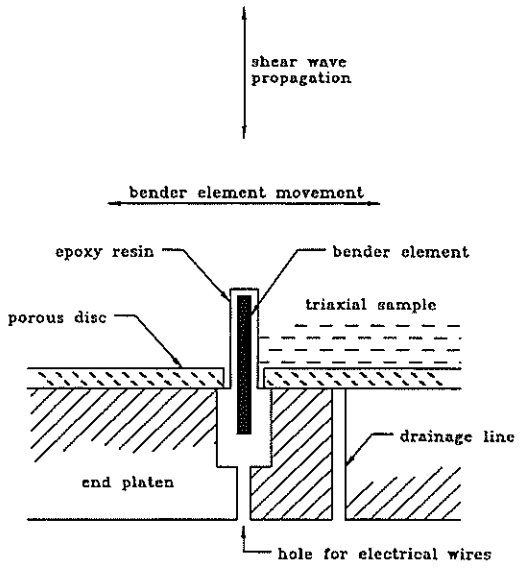

Figure 3 - Bender element mounting in triaxial cell

Electrical wires connected to the bender elements were sealed in the end platens and exited the triaxial cell using pressure resistant fittings.

The bender elements were configured such that the top element could act as a transmitter and the bottom element as a receiver. Using a function generator, an electrical signal was sent to the transmitter element and the time interval until arrival at the receiver element was measured using an oscilloscope, as shown in Figure 4.

INTERPRETATION OF BENDER ELEMENT RESULTS

Initial interpretation of bender element results is relatively straight-forward. To determine the velocity of a particle in motion (or a wave) it is necessary to know the time required for the particle to travel through a known distance. Previous test results (Viggiani and Atkinson [9], Nishihara [4]) have shown that for bender element testing the distance through which the first arrival waves travel, is the length between the tips of the bender elements. This length is commonly referred to as the *tip length* or *effective length*. The time required for the waves to travel through the effective length can be assessed as the time interval between sending the input signal to the transmitter element and the point of first arrival of the attenuated waveform at the receiver element.

Figure 5 shows an idealised trace record taken from an oscilloscope. From this trace it can be observed that an initial pulse is sent to the transmitter at time, t_0, and the first arrival wave is recorded at the receiver at time, t_1. The body wave velocities, v_p and v_s, can then be defined as:

$$v_p \text{ or } v_s = {}^{l_e}/_{\Delta t} \qquad (5)$$

where l_e is the effective or tip length and $\Delta t = (t_1 - t_0)$.

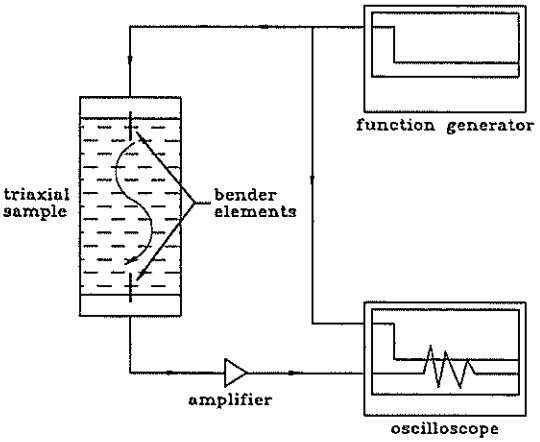

Figure 4 - Schematic representation of equipment used for bender element tests

The above method of determining body wave velocities is based on visual estimation of the time of arrival at the receiver element. This is the most commonly used method to calculate seismic wave velocities and is termed the method of *direct times of arrival*. Body wave velocities presented in this paper were determined using this method. Other methods include interval times of arrival, methods based on the cross-correlation function and methods based on dispersion curves obtained from the cross spectrum or transfer function. Viggiani and Atkinson [9], Mancuso, Simonelli and Vinale [3], and Sánchez-Salinero, Roesset and Stokoe [5] present further information on these methods of analysis.

DIFFICULTIES ASSOCIATED WITH BENDER ELEMENT TESTING

Figure 5 is a rather idealised presentation of actual bender element results. Whilst there is general agreement that the effective wave path length is the tip length of the specimen, determination of the point of first arrival is rather more subjective, as highlighted in Figures 6 and 7. Visual methods of estimating arrival times require a degree of judgement by the observer, which is unlikely to produce exact solutions for body wave velocities. The development of mathematical/analytical methods for determining arrival times can produce solutions which are more accurate than those determined by visual methods, though it should be noted that analytical methods were developed primarily for in situ seismic testing which usually incorporate more than one receiver.

Near-Field Effects

Analytical studies by Sánchez-Salinero, Roesset and Stokoe [5] have shown that for two-dimensional in-plane

(SV-motion) and three-dimensional elasto-dynamic motion two types of body waves were present in the waveform solutions. One wave travelled at the P-wave velocity, the other at the S-wave velocity. It was observed that for S-wave excitation the amplitude of the P-wave attenuated much faster than the dominant S-wave. It was concluded that the P-wave was only significant at distances which were 'close' to the source and is commonly referred to as the *near-field wave*. The S-wave in this case is referred to as the far-field wave. Similarly, for P-wave excitation, a near-field S-wave and a far-field P-wave were observed. When the direction of the excitation impulse is reversed both the near- and far-field terms change polarity.

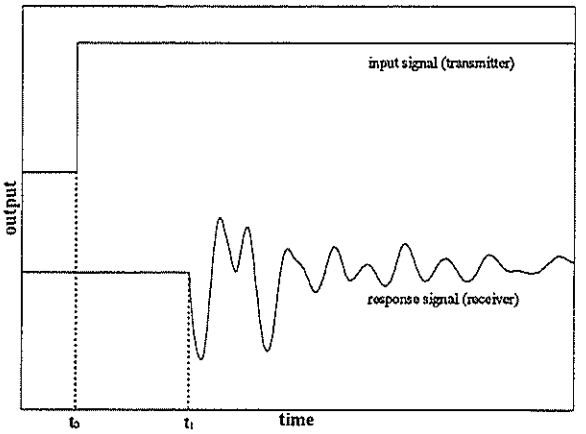

Figure 5 - Idealised bender element trace record

The orientation of the bender element shown in Figure 3, is such that the element is effectively a cantilever surrounded by soil. When the bender element is excited, this configuration results in shear waves emanating from the element and propagating through the soil in a direction parallel to the axis of the specimen, ie SH-waves. Considering a bender element test of a triaxial sample in three-dimensions, it is expected that a near-field P-wave will be present. The effect of this near-field wave varies, though in general, can mask the arrival of the shear wave.

EXPERIMENTAL TEST PROCEDURES

The results presented in this paper were obtained from tests performed on samples contained in conventional triaxial cells. All samples were in their natural (undisturbed) state, typically 76mm in diameter and 152mm in length. Bender elements were installed in the top and bottom platens, as described previously. It was necessary to pre-cut a fine slot in each end of the sample to facilitate insertion of the bender elements without damage. The bender element tests were performed on the samples immediately following the consolidation stage.

The equipment used in each bender element test included a Yokogawa FG110 2MHz synthesised function generator and a Yokogawa DL1200A 4 channel 100MHz digital oscilloscope. It was necessary to incorporate an amplifier (gain=56) to improve readability of the output signal. From previous testing it was also observed that earthing the sample similarly improved the signal output. The polarity of the input signal was reversed to assist determination of wave arrival times.

The oscilloscope permitted direct reading of time intervals using on-screen measurement cursors. Additionally, many signal traces were down-loaded directly from the oscilloscope to a personal computer for later analysis. The maximum resolution of down-loaded signals was 10000 points per trace.

TEST RESULTS

Bender element tests were performed on four undisturbed samples of different soil type. Sample descriptions and a summary of soil properties are detailed in Table 1. A series of tests were performed on each sample utilising a square pulse with an amplitude in the range of ±4V to ±20V as an input signal. The frequency of the square pulse was 10Hz. Figures 6 and 7 show bender element trace records for sample 1. All wave velocities were determined using the method of direct times of arrival and the tip length of each specimen

Figures 6 and 7 show very different first arrival times, 0.99ms and 0.18ms respectively. Considering the theory of near field effects, it is apparent that the these arrival times correspond to T_s and T_p respectively. Reversal of the polarity of the input signal reverses the output for both frequencies tested. Table 2 summarises arrival times and wave velocities for the square input wave.

Using equations (2), (4) and (3), the dynamic elastic parameters G_{max}, E and ν can calculated for the square impulse, as shown in Table 3. The undrained shear strength, s_u, for each sample, was measured using a consolidated undrained triaxial test. A loading rate of 10% axial strain per hour was adopted for all tests. Table 3 shows a summary of measured undrained shear strengths.

Table 1 - Summary of sample properties

Sample No.	Soil Description	Sample Depth (m)	Water Content (%)	Bulk Density (kg/m^3)
1	Firm light brown silty CLAY (Waitemata Series)	2.7	48.4	1680
2	Soft dark grey CLAY with black organic material	2.9	52.3	1640
3	Firm dark brown clayey SILT with coarse sand intermixed	2.0	53.9	1480
4	Firm light brown silty fine SAND with occasional pumice sand intermixed	5.1	50.4	1620

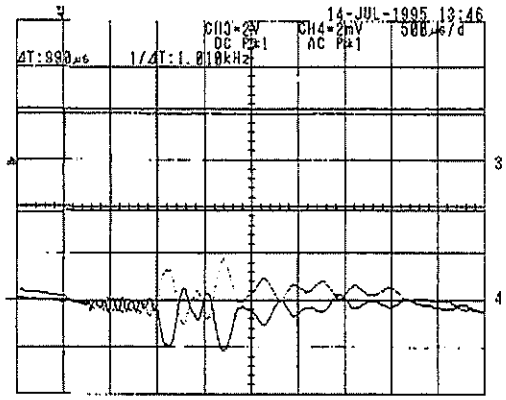

Figure 6 - Square impulse 10Hz (0.5ms/div)

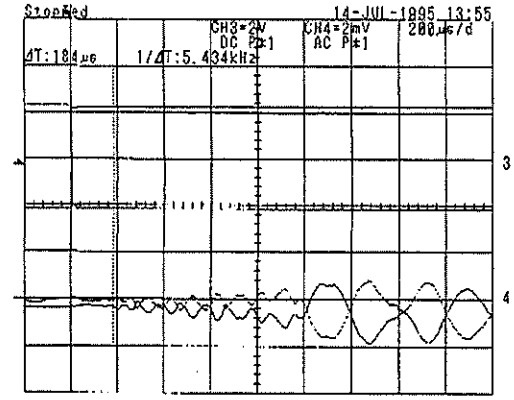

Figure 7 - Square impulse 10Hz (0.2ms/div)

Table 2 - Body wave velocities (square impulse)

Sample No.	Confining Pressure (kPa)	T_p (ms)	T_s (ms)	v_p (m/s)	v_s (m/s)
1	27	0.18	0.99	783	143
2	30	0.14	2.05	949	65
3	20	0.17	1.08	762	120
4	53	0.21	1.09	613	118

Table 3 - Elastic soil parameters (square impulse)

Sample No.	G_{max} (MPa)	E (MPa)	ν	s_u (kPa)
1	34.0	100.8	0.483	60
2	6.9	20.7	0.498	22
3	21.3	63.3	0.487	138
4	22.6	66.9	0.481	412

DISCUSSION AND CONCLUSIONS

The results have shown that it is possible to measure both P- and S-wave velocities using bender elements mounted in a triaxial cell. Knowledge of both these velocities enable the dynamic elastic parameters G_{max}, E and ν to be calculated. For the tests presented in this paper, ν values greater than 0.48 were calculated for all samples, indicating that bender element tests can be modelled essentially in an undrained manner.

The P-wave velocity measured in these tests is likely to be the velocity of the near-field P-wave associated with primary SH-wave motion in three dimensional space, as described by Sánchez-Salinero, Roesset and Stokoe [5]. To measure the P-wave velocity of a soil, it is best to use a source rich in P-waves and not rely upon a near field P-wave. However, the results for the square impulse presented in this paper, indicate that v_p can be consistently measured with reasonable accuracy, enabling elastic parameters for a soil specimen to be obtained quickly from a bender element test.

The use of a sine pulse as an input signal was investigated, however it was observed that the sine impulse demonstrated the frequency dependent response of the soil. This response is to be expected, as a input signal will impart energy to the specimen with a frequency range dominated by the frequency of the input signal. Consequently, it was easier to observe the higher frequency P-wave response of the soil by testing with a higher frequency sine impulse. The square input wave, on the other-hand, has a very wide range of input frequencies, enabling P- and S-waves to observed independently of the frequency of the input signal. The sharp fronted wave induced by the square impulse provides output similar to that observed from in situ seismic tests (Stokoe and Woods [7]), with better wave discrimination than that produced by the sine impulse. For

these reasons, it can be concluded that, in general, the square input wave provides the clearest bender element response.

The elastic parameters calculated for each specimen show general agreement with soil type; G_{max} tending to increase with s_u. It should be noted that s_u for samples 3 and 4 (sandy samples) were associated with large negative pore water pressures. Considering samples 1 and 2 (clays) only, G_{max} is of the order of 300 to 600 times s_u. In comparison, Seed and Idriss [6] present in situ test results where G_{max} ranges from approximately 1000 to 5000 times s_u. This would indicate that the G_{max} values determined from the bender element tests may be low. Several factors may contribute to this discrepancy and include sample disturbance, soil anisotropy and confining pressure.

Some sampling disturbance is inevitable with laboratory testing of 'undisturbed' soil samples. The implications of sample disturbance on bender element testing is not well documented, though any damage to a specimen would most likely result in a reduction of G_{max}. This reduction would be dependent on the degree of sample disturbance. The effects of soil anisotropy are discussed by Sully and Campanella [8], who highlight that in situ crosshole and downhole seismic tests may yield different shear wave velocities. It was concluded that this variation in velocity with test direction could provide an indicator to structural anisotropy of the soil. The variation of G_{max} with confining pressure has been well documented (Viggiani and Atkinson [10]), and in general, G_{max} approximately varies with confining pressure raised to the power of 1/3 to 1/2.

It should be noted that the in situ test results presented by Seed and Idriss [6] do not account for the effect of either soil anisotropy or confining pressure, thus direct comparisons of these results with those from bender element tests may not be accurate. In any case, it is apparent that further research into the use of bender elements to determine dynamic soil properties is required, particularly for soils in their natural state.

ACKNOWLEDGMENTS

The authors are grateful Mr. G. C. Duske for setting up the equipment necessary to perform the bender element tests, and Dr. T. J. Larkin for providing assistance with interpretation of test results.

REFERENCES

1. Abbiss, C. P., 1981, Shear wave velocity measurements of the elasticity of the ground, *Geotechnique* 31(1): 91-104.
2. Dyvik, R. and Madshus, C., 1985, *Lab measurements of G_{max} using bender elements*, Advances in the Art of Testing Soils Under Cyclic Conditions, Proceedings of a session of the ASCE Convention, Detroit, pp. 186-196.
3. Mancuso, C., Simonelli, A. L. and Vinale, F., 1989, *Numerical analysis of in situ S-wave measurements*, Proceedings of the 12th International Conference on Soil Mechanics, Vol. 3, pp.277-280.
4. Nishihara, A., 1993, Unpublished laboratory work.
5. Sánchez-Salinero, I., Roesset, J. M. and Stokoe II, K. H., 1986, *Analytical studies of body wave propagation and attenuation*, Report GR86-15, The University of Texas at Austin.
6. Seed, H. B. and Idriss, I. M., 1970, *Soil Moduli and damping factors for dynamic response analysis*, Report No. EERC 70-10, Earthquake Engineering Research Centre, University of California, Berkeley, California.
7. Stokoe, K. H. and Woods, R. D., 1972, In situ shear wave velocity by cross-hole method, *ASCE Journal of the Soil Mechanics and Foundations Division* 98(SM 5): 443-460.
8. Sully, J. P. and Campanella, R. G., 1995, Evaluation of in situ anisotropy from crosshole and downhole shear wave velocity measurements, *Geotechnique* 45(2): 267-282.
9. Viggiani, G. and Atkinson, J. H., 1995, Interpretation of bender element tests, *Geotechnique* 45(1): 149-154.
10. Viggiani, G. and Atkinson, J. H., 1995, Stiffness of fine-grained soil at very small strains, *Geotechnique* 45(2): 249-265.